Enhancing Vulnerable Road User Detection and Volumetric Data Through Advanced Infrastructure Detection Technologies

January 2025

Publication No. FHWA-HRT-24-175

U.S. Department of Transportation
Federal Highway Administration

Research, Development, and Technology
Turner-Fairbank Highway Research Center
6300 Georgetown Pike McLean, VA 22101-2296

Turner-Fairbank
Highway Research Center

FOREWORD

Advanced infrastructure-based detection technologies, such as infrared thermal imaging sensors, light detection and ranging (LiDAR), and radar, have the potential to improve vulnerable road user detection and vulnerable road user volumetric data collected at real world intersections and midblock crossings. This improved volumetric data can help provide researchers and government agencies with a better understanding of roadway usage and vulnerable road user exposure to crash risk. This understanding can provide insight into which intersections and midblock crossings have the greatest potential risks to various kinds of vulnerable road users and thus require the most intervention to reduce the risk of crashes, potentially reducing the total number of fatalities and injuries to vulnerable road users.

The current study sought to evaluate the strengths and weaknesses of two of these types of sensors. The research team evaluated infrared thermal imaging sensors and LiDAR sensors and then compared the two sensor types. This report may be of interest to State and local transportation agencies when planning to implement infrastructure-based vulnerable road user detection technologies at intersections and midblock crossings to reduce injuries and fatalities involving vulnerable road users.

John A. Harding
Director, Office of Safety and Operations
Research and Development

Notice

This document is disseminated under the sponsorship of the U.S. Department of Transportation (USDOT) in the interest of information exchange. The U.S. Government assumes no liability for the use of the information contained in this document.

Non-Binding Contents

Except for the statutes and regulations cited, the contents of this document do not have the force and effect of law and are not meant to bind the States or the public in any way. This document is intended only to provide information regarding existing requirements under the law or agency policies.

Quality Assurance Statement

The Federal Highway Administration (FHWA) provides high-quality information to serve Government, industry, and the public in a manner that promotes public understanding. Standards and policies are used to ensure and maximize the quality, objectivity, utility, and integrity of its information. FHWA periodically reviews quality issues and adjusts its programs and processes to ensure continuous quality improvement.

Disclaimer for Product Names and Manufacturers

The U.S. Government does not endorse products or manufacturers. Trademarks or manufacturers' names appear in this document only because they are considered essential to the objective of the document. They are included for informational purposes only and are not intended to reflect a preference, approval, or endorsement of any one product or entity.

Recommended citation: Federal Highway Administration, *Enhancing Vulnerable Road User Detection and Volumetric Data Through Advanced Infrastructure Detection Technologies* (Washington, DC: 2024) https://doi.org/10.21949/1521784

TECHNICAL REPORT DOCUMENTATION PAGE

1. Report No. FHWA-HRT-24-175	2. Government Accession No.	3. Recipient's Catalog No.	
4. Title and Subtitle Enhancing Vulnerable Road User Detection and Volumetric Data Through Advanced Infrastructure Detection Technologies		5. Report Date January 2025	
		6. Performing Organization Code: HRSO-30	
7. Author(s) Jose Calvo, Yi-Ching Lee, Evan Bowden, Mafruhatul Jannat, and Jesse Eisert		8. Performing Organization Report No.	
9. Performing Organization Name and Address Leidos, Inc 1750 Presidents Street Reston, VA 20190		10. Work Unit No.	
		11. Contract or Grant No. 693JJ319D000012	
12. Sponsoring Agency Name and Address Office of Safety and Operations Research and Development Federal Highway Administration 6300 Georgetown Pike McLean, VA 22101-2296		13. Type of Report and Period Covered Technical Report: XX XXXX–March 2025.	
		14. Sponsoring Agency Code HRSO-30	
15. Supplementary Notes The Contracting Officer's Representative is Jesse Eisert.			

16. Abstract

Advanced, infrastructure-based detection technologies, such as infrared thermal imaging sensors and Light Detection and Ranging (LiDAR), can potentially improve vulnerable road user detection and vulnerable road user volumetric data collection at real-world intersections and midblock crossings. These technologies can help increase understanding of roadway usage and vulnerable road user exposure to crash risk and help researchers identify the intersections with the greatest risk to various vulnerable road users and the intersections and midblock crossings that most need intervention to reduce vulnerable road user crash risk, fatalities, and injuries. The research initiative detailed in this report investigated infrared thermal imaging sensors and LiDAR sensors to determine strengths, weaknesses, overall abilities, and applicability in real-world settings, assessing each sensor independently. The research team first evaluated the thermal sensors and then the LiDAR sensors. Then, based on the data collection process, the research team made two comparisons, comparing the performance of the thermal sensors across two time points and the performance of the second round of thermal sensors to the LiDAR sensors. The thermal sensors performed better than the LiDAR sensors overall and had better detection rates. Additionally, the performance of the thermal sensors was better in study 1 (the thermal sensor evaluation) than in study 2 (the LiDAR sensor evaluation and thermal-LiDAR sensor comparison). Both sensors were able to detect vulnerable road users at night, which is a strength. However, neither sensor was able to successfully detect all the pedestrians in a cluster of three pedestrians. While both sensors were able to detect vulnerable road users at both midblock crossings and at intersections, based on the results, a possible conclusion is that positioning and placement of the sensors influences the performance of both types of sensors. These technologies advance and evolve at a rapid pace, and further research on the next generation of these sensors is needed to evaluate their ability and applicability in real-world circumstances.

17. Key Words Pedestrian detection, pedestrian safety, vulnerable road users, bicyclists, infrared thermal imaging sensors, LiDAR sensors	18. Distribution Statement No restrictions. This document is available to the public through the National Technical Information Service, Springfield, VA 22161. https://www.ntis.gov

19. Security Classif. (of this report) Unclassified	20. Security Classif. (of this page) Unclassified	21. No. of Pages 50	22. Price N/A

Form DOT F 1700.7 (8-72) Reproduction of completed page authorized.

SI* (MODERN METRIC) CONVERSION FACTORS

APPROXIMATE CONVERSIONS TO SI UNITS

Symbol	When You Know	Multiply By	To Find	Symbol
		LENGTH		
in	inches	25.4	millimeters	mm
ft	feet	0.305	meters	m
yd	yards	0.914	meters	m
mi	miles	1.61	kilometers	km
		AREA		
in^2	square inches	645.2	square millimeters	mm^2
ft^2	square feet	0.093	square meters	m^2
yd^2	square yard	0.836	square meters	m^2
ac	acres	0.405	hectares	ha
mi^2	square miles	2.59	square kilometers	km^2
		VOLUME		
fl oz	fluid ounces	29.57	milliliters	mL
gal	gallons	3.785	liters	L
ft^3	cubic feet	0.028	cubic meters	m^3
yd^3	cubic yards	0.765	cubic meters	m^3
	NOTE: volumes greater than 1,000 L shall be shown in m^3			
		MASS		
oz	ounces	28.35	grams	g
lb	pounds	0.454	kilograms	kg
T	short tons (2,000 lb)	0.907	megagrams (or "metric ton")	Mg (or "t")
		TEMPERATURE (exact degrees)		
°F	Fahrenheit	5 (F-32)/9 or (F-32)/1.8	Celsius	°C
		ILLUMINATION		
fc	foot-candles	10.76	lux	lx
fl	foot-Lamberts	3.426	$candela/m^2$	cd/m^2
		FORCE and PRESSURE or STRESS		
lbf	poundforce	4.45	newtons	N
lbf/in^2	poundforce per square inch	6.89	kilopascals	kPa

APPROXIMATE CONVERSIONS FROM SI UNITS

Symbol	When You Know	Multiply By	To Find	Symbol
		LENGTH		
mm	millimeters	0.039	inches	in
m	meters	3.28	feet	ft
m	meters	1.09	yards	yd
km	kilometers	0.621	miles	mi
		AREA		
mm^2	square millimeters	0.0016	square inches	in^2
m^2	square meters	10.764	square feet	ft^2
m^2	square meters	1.195	square yards	yd^2
ha	hectares	2.47	acres	ac
km^2	square kilometers	0.386	square miles	mi^2
		VOLUME		
mL	milliliters	0.034	fluid ounces	fl oz
L	liters	0.264	gallons	gal
m^3	cubic meters	35.314	cubic feet	ft^3
m^3	cubic meters	1.307	cubic yards	yd^3
		MASS		
g	grams	0.035	ounces	oz
kg	kilograms	2.202	pounds	lb
Mg (or "t")	megagrams (or "metric ton")	1.103	short tons (2,000 lb)	T
		TEMPERATURE (exact degrees)		
°C	Celsius	1.8C+32	Fahrenheit	°F
		ILLUMINATION		
lx	lux	0.0929	foot-candles	fc
cd/m^2	candela/m2	0.2919	foot-Lamberts	fl
		FORCE and PRESSURE or STRESS		
N	newtons	2.225	poundforce	lbf
kPa	kilopascals	0.145	poundforce per square inch	lbf/in^2

*SI is the symbol for International System of Units. Appropriate rounding should be made to comply with Section 4 of ASTM E380. (Revised March 2003)

TABLE OF CONTENTS

LIST OF FIGURES

LIST OF TABLES

LIST OF ABBREVIATIONS

CCTV	closed-circuit television
CDA	cooperative driving automation
DVR	digital video recorder
FHWA	Federal Highway Administration
FOV	field of view
LiDAR	light detection and ranging
NCSA	National Center for Statistics and Analysis
OEM	original equipment manufacturer
TFHRC	Turner-Fairbank Highway Research Institute

CHAPTER 1. INTRODUCTION

INTRODUCTION

According to the National Highway Traffic Safety Administration, 7,522 pedestrian deaths and 1,105 pedalcyclist deaths occurred in 2022, and nonoccupants of vehicles accounted for 21 percent of all traffic fatalities (National Center for Statistics and Analysis (NCSA) 2024b, 2024a). About two-thirds of pedestrian fatalities occurred after dark (77 percent), 20 percent during daylight hours, 2 percent at dusk, and 2 percent at dawn. About half of pedalcyclist fatalities occurred after dark (52 percent), 44 percent during daylight hours, and 4 percent at dusk or dawn. In terms of locations, 16 percent of pedestrian fatalities and 29 percent of pedalcyclist fatalities occurred at intersections. Most of these fatalities (84 percent of pedestrians and 85 percent of pedalcyclists) occurred in urban, not rural, areas.

Vulnerable road users are at greater risk of serious injury or death if they are involved in a traffic crash (Organisation for Economic Co-operation and Development 1998). According to Walker (2022), the Federal Highway Administration (FHWA) says:

> A vulnerable road user is a nonmotorist with a fatality analysis reporting system (FARS) person attribute code of pedestrian, bicyclist, other cyclist, person on personal conveyance, or injured person who is or is equivalent to a pedestrian or pedalcyclist as defined in the ANSI [American National Standards Institute] D16.1-2007 (National Safety Council 2007). See U.S. Code (U.S.C.) 23 §148(a)(15) and Code of Federal Regulations (CFR) 23 924.3 §490.205 [GPO 2024a, 2024b]. A vulnerable road user may include people walking, biking, or rolling. Please note that a vulnerable road user:
>
> - Includes a highway worker on foot in a work zone, given they are considered a pedestrian.
> - Does not include a motorcyclist.

The challenges associated with collecting nonmotorized data are well documented. FHWA's *Traffic Monitoring Guide* and the National Cooperative Highway Research Program's (NCHRP) *NCHRP Report 797: Guidebook on Pedestrian and Bicycle Volume Data Collection* outline several of those challenges (FHWA 2016; Ryus et al. 2014).

Researchers have discussed measuring pedestrian exposure to crash risk for more than three decades, but a consensus on an effective method for measuring exposure remains elusive. In part, this dissonance is due to the challenges associated with collecting pedestrian data (FHWA 2016). For example, vulnerable road users traverse paths that are less confined than fixed lanes, take shortcuts off sidewalks in unmarked crossing locations, and often travel in closely spaced groups—making it difficult for sensors to differentiate among individuals within the group. Additionally, vulnerable road users are harder to detect at night than during the day.

Advancements in sensing and data mining techniques—combined with high-performance computing resources—facilitated the development of several innovative approaches to detecting vulnerable road users in recent years. Researchers compared the benefits and drawbacks of

approaches that are both vehicle-based (e.g., on-board cameras, radar, global positioning system, accelerometers) and infrastructure-based (e.g., roadway cameras, light detection and ranging (LiDAR), radar, thermal imaging, ultrasonic, sensor fusion) (Reyes-Muñoz and Guerrero-Ibáñez 2022; Vargas et al. 2021). For example, time-to-collision or post-encroachment-time, in the context of vehicle-pedestrian conflicts, can be calculated from roadway cameras, which is a benefit (Ismail et al. 2009).

On the other hand, video-based sensor performance can be compromised by lighting conditions, obstacles, and weather conditions (Lv et al. 2019). To overcome these performance limitations, researchers explored the use of other sensors for the detection of vulnerable road users and objects. Liu et al. (2021) proposed a thermal infrared pedestrian detection method for detecting and classifying motion-blurred, tiny, and dense objects. The researchers used infrared images collected through vehicle-mounted infrared thermal image detectors in complex scenarios on highways and roads. Results showed the proposed approach achieved a 72-percent accuracy score for detecting standing and walking pedestrians.

Ansariyar and Jeihani (2023) installed LiDAR sensors at an intersection in Baltimore, MD, and evaluated the sensors' capability, in conjunction with a machine-learning algorithm, to detect vehicle-bicycle conflicts while considering time of day, traffic signal phase, and weather conditions. Results showed this approach could detect vehicle-bicycle conflicts over several months, the severity of conflicts based on the speed and heading of the vehicle and bicycle, and conflict frequency at the intersection. Researchers observed more conflicts after 5 p.m. and determined the conflicts were more severe on sunny days than cloudy or rainy days.

In another field study, researchers implemented LiDAR sensors at an intersection in Reno, NV to detect vehicle-pedestrian conflicts (Lv et al. 2019). Using a trajectory extraction analysis, Lv et al. determined that the proposed approach could identify vehicle-pedestrian near-crash events, but they noted some misidentifications due to inconsistencies in the distances between vehicles and pedestrians, vehicle speed, deceleration, and driver-reaction time.

Other studies investigated detecting static pedestrians and animals using two-dimensional LiDAR, a red-green-blue camera, and a calibration technique that connected two sensors and an object-detection algorithm (Khaled et al. 2023). Additionally, Zhao et al (2019) studied predicting pedestrian crossing intentions by using pedestrian trajectories and walking behaviors. A recent field evaluation of smart city sensor deployment—including sensors mounted inside vehicles (e.g., forward collision warning) carried by the vulnerable road users (e.g., smartphones and smartwatches) and installed on infrastructure (e.g. video cameras, radar, LiDAR)—showed that potential pedestrian-vehicle conflicts could be detected prior to when the collision would be considered unavoidable (Teixeira et al. 2023). The level of detection accuracy depended on the sensor's capability to track vehicle and pedestrian locations and compute data fusion. However, testing was conducted during the day and with one single walking pedestrian only.

Most prior studies focused on the detection of pedestrians and bicyclists. Advanced detection systems must be able to detect different types of vulnerable road users, including scooter riders and wheelchair users. For example, the number of electronic scooter systems implemented in North American cities from 2020 to 2021 increased by 30 percent (North American Bikeshare and Scootershare Association 2022). As scooter activity increases, transportation agencies must

install systems that can accurately detect these types of vulnerable road users. Furthermore, in consideration of exposure to crash risk, including all individuals is important. If sensors cannot identify certain types of vulnerable road users, such as wheelchair users, the calculation of exposure would be misrepresented based on missing an entire subpopulation.

In calculations of exposure to crash risk, pedestrians of all ages must also be considered. For example, studies have shown that child pedestrians are at higher risk of collision with motor vehicles than adults—especially at midblock crossings (Rothman et al. 2012). In 2022, 5 percent of all pedalcyclists killed and 15 percent of all pedalcyclists injured were children age 14 and younger (NCSA 2024a). Meanwhile, 2 percent of all pedestrians killed and 10 percent of all pedestrians injured were children 14 and younger (NCSA 2024b). Few studies to date have examined the ability of advanced detection systems to sense children and adults with equal accuracy—even though crash data on child pedestrians are available (NCSA 2023b; Rothman et al. 2012),

To advance research into viable methods for improving vulnerable road user safety, FHWA developed a vulnerable road user technology test bed at Turner-Fairbank Highway Research Center (TFHRC) (FHWA n.d.). The test bed examines technologies and sensors that support pedestrian and bicyclist system concepts, standards, and applications and related product innovations (Jannat et al. 2021). FHWA installed nine infrared thermal imaging sensors in the test bed and calibrated the sensors to accurately detect vehicles, pedestrians, and bicyclists on the testbed.

Additionally, the thermal and LiDAR sensors did not need light to detect various road users (Jannat et al. 2021). Better understanding the ability—and applicability—of these sensors under various conditions can potentially help State and local departments of transportation decide whether to implement sensors for safety initiatives or if count data from infrared thermal imaging sensors can calculate pedestrian exposure.

OBJECTIVES

The purpose of this research was to evaluate the appropriateness and applicability of both infrared thermal imaging sensors and LiDAR sensors for collecting vulnerable road user count data—under variable conditions—that can provide information for measuring exposure to crash risk. The research team tested the infrared thermal imaging sensor's ability to detect the following:

- Single pedestrians in two scenarios for LiDAR and three scenarios for thermal:
  - Adult.
  - Heavily clothed pedestrian (thermal sensors only)
  - Child (as represented by a child pedestrian articulating dummy).
- Multiple adult pedestrians.
- Bicyclists.
- Scooter users.
- Wheelchair users.

Testing occurred under different conditions, including light, dark, slow crossing, fast crossing, and crossing location.

CHAPTER 2. INFRARED THERMAL IMAGING SENSORS

This study investigated the ability and applicability of infrared thermal imaging sensors to detect vulnerable road users and provide accurate vulnerable road user volumetric data. The research team selected seven different vulnerable road user types: a single pedestrian, a group of three pedestrians, a bicyclist, an electric scooter user, a wheelchair user, a child pedestrian, and a single pedestrian in heavy clothing. These vulnerable road user types were observed during the day in full daylight and at night under minimal lighting conditions. Additionally, the crossings of the vulnerable road users were assessed both at an intersection crossing and a midblock crossing. Finally, the vulnerable road users crossed at both slower and higher speeds based on vulnerable road user type.

METHOD

Apparatus

The following subsections describe the technologies and testbed used and analyzed in this study.

TFHRC Vulnerable Road User Technology Test Bed

The research team conducted testing on the TFHRC vulnerable road user technology test bed. The test bed comprises two marked, signalized intersections with pedestrian crosswalks; signal heads and call buttons; and one marked midblock crossing along a two-lane, two-way, 22-ft-wide road.

Infrared Thermal Sensors

The research team selected four thermal imaging sensors located on the TFHRC vulnerable road user technology test bed. Two of the sensors have a detection distance of 6–100 ft, with fields of view (FOVs) measuring 90° horizontally and 69° vertically. The other two sensors have detection distances ranging from 32–245 ft, with FOVs measuring 45° horizontally and 35° vertically. All four infrared thermal imaging sensors are long-wave infrared (7–14 μm). They have capabilities for vehicle and bicycle presence detection, vehicle and bicycle counting, pedestrian counting, traffic data collection, and traffic flow monitoring. The sensors have three primary types of detection zones: vehicle, bicycle, and pedestrian. Detection zones are designated areas within a sensor's FOV. The detection zones can be applied in the graphical user interface of the infrared thermal imaging sensor's software. Detection zones outline an area meant to detect specific entities traversing through the zones.

The sensors are designed to track and measure the size of any thermal signature they can see within their FOV based on the detection algorithm the OEM developed. When a thermal signature moves into a designated detection zone, the sensor determines whether the size of the thermal signature falls within the accepted size range for the type of detection zone being used (e.g., if set to a vehicle zone, a sensor would detect vehicles rather than bicyclists). When it detects, the sensor begins sending tracking data, which can then be recorded. Sensors transmit video, tracking, and count data across the network on which they are installed. Transmission of count data and thermal video data is continuous—regardless of whether a thermal signature is in

a detection zone—and the rate of transmission can be changed as needed. Every 10 s, the sensors transmit a message that includes the total number of thermal signatures detected in each zone during that 10-s period. A signature enters a detection zone and then is counted in the cycle after it leaves that zone. The output of the count data also includes a classifier of the entity being detected, based on the kind of detection zone used: vehicle, bicycle, or pedestrian.

The research team defined pedestrian detection zones for all crosswalks within the FOV of the selected sensors when setting up the thermal sensors and used only data from the zones located at the selected crosswalks. For this study, the research team set the devices to the pedestrian detection zone setting—both because the pedestrian detection zone setting could detect pedestrians, bicyclists, and other vulnerable road user types (according to the user manual) and because the bicycle detection zone setting reportedly detects only bicycles and ignores all other cross traffic. The bicycle setting is primarily for use in designated bicycle areas on roadways. In addition, the user manual for the sensors and system noted that pedestrian sensors and bicycle sensors should not be used at the same location.

The sensors were set up along Innovation Drive on the TFHRC campus, as shown in figure 1. Each sensor was set up to observe a primary crosswalk within the TFHRC test bed. Some of the sensors had multiple crosswalks in their FOVs; however, the ability to detect entities within secondary crosswalks outside each sensor's primary crosswalk depended on the sensor's placement angle and distance from the secondary crosswalks. Figure 1 shows the general locations and primary focal crosswalk of each sensor. Each focal crosswalk was located within the OEM-determined FOV and detection distance of its designated sensor.

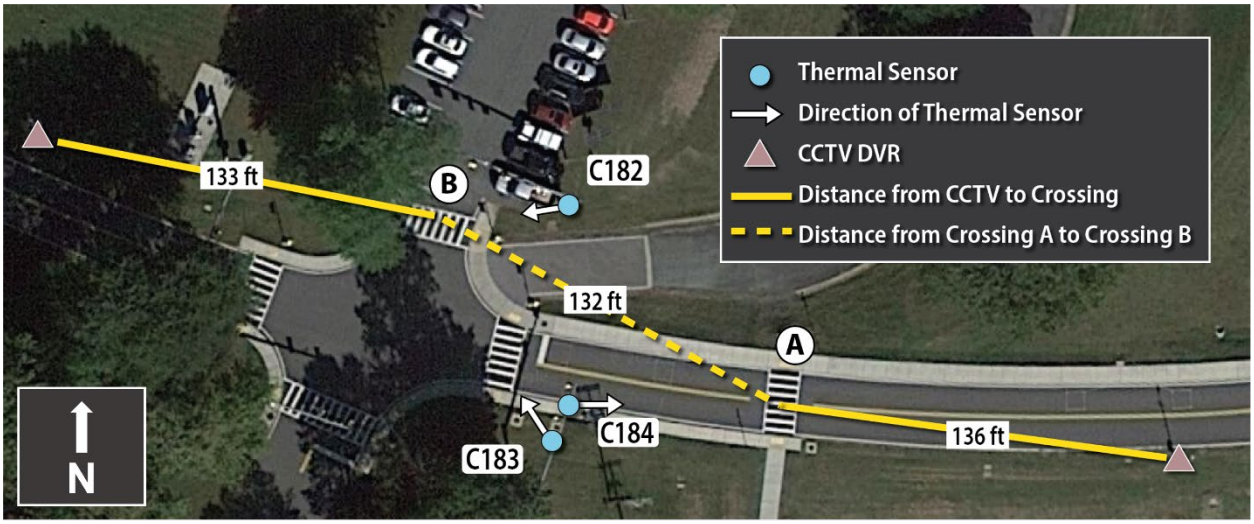

Original photo © 2023 Google® Earth™. Modified by FHWA (see Acknowledgments section).
CCTV = closed-circuit television; DVR = digital video recorder.

Figure 1. Photo. TFHRC test bed with infrared thermal imaging sensors, crosswalk, and CCTV DVR locations and distances.

Closed-Circuit Television (CCTV) Digital Video Recorders (DVRs)

The research team used two traditional CCTV DVRs to record a live, high-resolution video feed in color during data collection. The CCTV DVRs were located 133 ft and 136 ft from the intersection and midblock crossings, respectively. The DVRs were zoomed in to clearly see vulnerable road user activity on the testing site. The video feed kept a record of the ground truth motion of vulnerable road users during testing. The video was then compared with the video output of the infrared thermal imaging sensors to verify the quality of the infrared thermal imaging sensor recording.

Video Recording Software

The research team used an open-source video recording software to record live video streams of both the infrared thermal imaging sensors and the CCTV DVRs used in this study. The output included specific placement of the detection zones, which lit up when the sensor detected an entity of the appropriate type. The research team used video data to manually code detections when the count data failed to save properly due to the research team's prematurely ending the saved count feed, which occurred less than 3 percent of the time.

Electric Scooter

The study used a 350-W electric scooter with a 36-V, 15-Ampere-hour battery. The user manual lists the scooter's top speed at 20 mph and load capacity as 220 lb.

Wheelchair

The study used a self-propelled wheelchair. The wheelchair was collapsible, had detachable leg rests, and had a load capacity of 300 lb. The leg rests were attached and used during testing.

Bicycle

The study used a 26-inch, manual-cruiser-style bicycle to represent bicyclists.

Belt-Driven Articulating Pedestrian Dummy

The research team used a programmable articulating pedestrian dummy to simulate a child vulnerable road user. The child pedestrian dummy is 45.5 inches tall, roughly the average height of a 6-yr-old child. Disposable heating pads were attached to the dummy to simulate the natural body heat of a human. The average temperature of the disposable heating pads is 140 °F. Pilot testing revealed that applying disposable heating pads to all or selected parts of the dummy (chest, upper arms, upper legs, and back) enabled the infrared thermal sensors to identify the dummy as its own thermal signature and to successfully count the dummy as a pedestrian.

Experimental Design

The research team reviewed existing literature and worked with the FHWA Office of Safety and Operations Research and Development Human Factors Team to identify factors needed to address the objectives for infrared thermal imaging sensors. Several unknowns appeared to exist regarding these sensors, such as whether wearing heavy, well-insulated clothing would inhibit the thermal sensors' ability to accurately detect an individual and whether multiple signatures of body heat in high-population-density clusters crossing the street could make it difficult for infrared thermal imaging sensors to differentiate among multiple pedestrians crossing at the same time. Additionally, whether electric scooter users can be identified within the detection fields of infrared thermal imaging sensors similar to pedestrians and how differences in the speeds of various vulnerable road user types might affect thermal sensors' ability to detect them.

Figure 1 showed the location of the infrared thermal imaging sensors in the intersection. The research team selected crosswalks A and B as the primary crosswalks to test the sensors because of the A and B positions and the number of sensors that can see those crosswalks. Crosswalk A (midblock crossing) was on a vertical curve. For data collection, the team initially chose four infrared thermal imaging sensors located on the TFHRC campus but excluded the data from one sensor from the results due to technical issues. The sensors included C181, C182, C183, and C184. Table 1 lists the sensors that cover crosswalks A and B. C181 was excluded from figure 1 because the data from C181 were not included in the results.

Table 1. Infrared thermal imaging sensor crosswalk direction.

Crosswalk	Sensor Identification
A	C184
B	C181, C182, and C183

Each infrared thermal imaging sensor is within the detection range, as defined by the OEM, of either the designated intersection or midblock crossing.

The research team conducted pilot testing for the sensors and setup. During piloting, the team tested each condition level (i.e., the characteristics of each condition to be tested) of each factor at least twice to ensure no major issues with the thermal sensor setup or study design. During pilot testing, the team determined that the desired values for fast user conditions for bicyclists and scooter users could not be met due to the roadway geometry of the TFHRC vulnerable road user technology test bed. Therefore, the speeds for the fast condition for these user groups were adjusted to account for this geometry. (See the speed subsection for additional detail.)

During pilot testing, the research team also identified the optimal configuration for the multiple-adult-pedestrian condition. Initially, the experiment anticipated having three pedestrians walk across the roadway in a straight line with about 1 inch of separation between them. During each of these pilot testing trials, however, the sensors failed to recognize the three shoulder-to-shoulder pedestrians. With the pedestrians in this formation, the thermal sensors never produced tracking data or any successful counts.

With the pedestrians in a two-and-one configuration (i.e., two side by side, followed by one adult pedestrian), the thermal sensors produced tracking data and count data but counted only two or one pedestrian in the detection zone. Therefore, the team chose the two-and-one configuration for this study because this configuration showed that the sensors were still active and working but that other potential limitations restricted the thermal sensors' abilities and accuracy. The team also chose this configuration to replicate a more unorganized configuration, wherein multiple pedestrians might typically cross a crosswalk in the real world. The research team identified four key factors for the study: vulnerable road user type, speed, time of day, and location. Table 2 shows the condition levels for each factor.

Table 2. Factors and condition levels.

Factor	Condition Level
Vulnerable road user type	Single adult pedestrian Heavily clothed pedestrian Child pedestrian dummy Wheelchair user Three adult pedestrians Bicyclist Scooter user
Speed	Slow Fast
Time of day	Day Night
Location	Intersection Midblock

Vulnerable Road User Type

The research team chose seven vulnerable road user types to evaluate the infrared thermal imaging sensors' ability to detect different vulnerable road users (table 2). El-Urfali et al. (2019) used the single-adult-pedestrian condition to test advanced detection technologies, and the single adult pedestrian condition served as a comparison point for the performance of the other vulnerable road user types. This study used the heavily clothed pedestrian level to determine whether the infrared thermal sensors could detect a pedestrian through the insulation of several layers of clothing. The heavily clothed pedestrian wore a shirt with a sweatshirt or light jacket, a heavy coat, gloves, a knit scarf, and a ski cap while crossing. The child pedestrian dummy simulated a child pedestrian, testing the sensors' ability to detect vulnerable road users of different sizes. The advanced detection system was positioned so that the dummy could enter and leave the detection zone moving in one direction. The study used the condition with three adult pedestrians for determining the sensors' ability to detect multiple entities crossing in a group. In addition to those four pedestrian types, the three other levels included an adult wheelchair user, an adult bicyclist, and an adult scooter user. The adult-wheelchair-user condition operated the wheelchair with the leg rests attached.

Speed

The research team established two levels of speed—slow and fast—for each vulnerable road user type. Table 3 outlines the speeds chosen for each vulnerable road user type. The principal investigator validated the speed from the live-tracking data during data collection.

Table 3. Fast and slow speeds for each vulnerable road user type.

Vulnerable Road User Type	Slow Speed (mph)	Fast Speed (mph)
Single adult pedestrian	2	5
Three adult pedestrians	2	5
Heavily clothed pedestrian	2	5
Wheelchair user	2	5
Child pedestrian dummy	2	5
Bicyclist	5	10
Scooter rider	5	10

Time of Day

The experiment used two levels—day and night—to test the sensors' ability to detect vulnerable road users under normal daylight conditions and at night, when there is no ambient sunlight. The research team defined "day" as any time during the period from at least 1 h after sunrise to 1 h before sundown each day. The team defined "night" as any time during the period from at least 1 h after sundown to 1 h before sunrise. The definitions meant that researchers conducted experiments during the day time-of-day level in full daylight and experiments during the night time-of-day level, when there was no light from the sun. Additionally, the research team collected ambient metadata, including weather (i.e., sunny, partly sunny, and cloudy), although researchers did not collect data during very cloudy or adverse weather.

Location

Two locations along the TFHRC vulnerable road user test bed were chosen for data collection: an intersection crosswalk and a midblock crosswalk. The intersection and midblock crossings can be seen in figure 1.

System Performance Metrics

This study's performance measures were true detection accuracy (recall), system accuracy (precision), and F1 score—a type of F-score that measures accuracy by using precision and recall. Because both the recall and the precision of advanced detection technologies are important, the study can use an F1 score. An F1 score measures accuracy and incorporates the proportion of hits compared with all trials (including misses) and all detections (including false positives), weighing those two aspects of accuracy equally.

Table 4 outlines the four potential outcomes for any single trial (i.e., detection or no detection) that occurred during data collection. Agencies use these potential outcomes to calculate the established performance metrics. True detection accuracy measures the thermal sensors' ability to detect vulnerable road users while also accounting for misses; for example, the sensor receives

a true detection accuracy rate of 50 percent if the sensor makes 5 successful detections out of 10 possible detections. System accuracy measures the thermal sensors' ability to detect only vulnerable road users and exclude nonvulnerable road users and false detections; for example, if a sensor makes a total of 10 detections but only 8 are accurate detections of actual vulnerable road users, leaving 2 false detections, the system accuracy rate is 80 percent.

Table 4. Outcomes for a single trial of data collection.

Vulnerable Road User Crossing	Sensor Output	Outcome
Crossing	Detection	Hit
Crossing	No detection	Miss
No crossing	Detection	False detection
No crossing	No detection	Correct rejection

The research team used true detection accuracy as a measure to determine the abilities of the sensors. The team used system accuracy in conjunction with true detection accuracy to calculate an F1 score. The team used the F1 score to assess the applicability of the thermal sensors for detecting vulnerable road users. The applicability of the sensors is based on sensor ability to detect vulnerable road users and on their ability to minimize false detections.

Figure 2 through figure 4 show equations for the chosen performance metrics.

$$\sum Hits/\left(\sum Hits + \sum Misses\right)$$

Figure 2. Equation. True detection accuracy.

$$\sum Hits/\left(\sum Hits + \sum False\ Detections\right)$$

Figure 3. Equation. System accuracy.

$$2\frac{(True\ detection\ accuracy * System\ accuracy)}{(True\ detection\ accuracy + System\ accuracy)}$$

Figure 4. Equation. F1 score.

The research team set the minimal acceptable F1 score for vulnerable road user detection as 0.85. Based on the work of El-Urfali et al. (2019), the team set the minimal acceptable F1 score as 0.85 and the minimal acceptable true detection accuracy as 85 percent. Any scores below those scores resulted in unacceptable performances (table 5).

Table 5. F1 score and true detection accuracy thresholds.

F1 Score	True Detection Accuracy (percent)	Rating
≥0.85	≥85	Acceptable performance
≤0.84	≤84	Unacceptable performance

The research team reviewed and analyzed the data to determine the infrared thermal imaging sensor's ability to detect pedestrians, bicyclists, and the other vulnerable road users at the intersection and marked midblock crossing at TFHRC in different conditions (e.g., light and dark, slow and fast crossings, congestion, heavy clothing). Based on a power analysis with a 95-percent confidence interval (±5 percent), the team tested each combination of the chosen factors six times each. Six trials for each of the 56 conditions, with 2 sensors at the intersection location and 1 at the midblock, resulted in a total of 504 observations. Collapsing the data across the various factors resulted in 72 observations for each level of vulnerable road user type, 252 observations for each level of speed, 252 observations for each level of time of day, 336 observations for the intersection level of location, and 168 observations for the midblock level of location.

The team executed a single crossing in each trial based on the parameters of the condition being examined, resulting in a single data point per sensor per trial. The data point then had a count of the total number of vulnerable road users the thermal sensors detected, enabling the research team to identify both misses and false detections.

Data collection occurred over 3 mo. Members of the research team acted as the adult vulnerable road users by moving through a designated intersection crosswalk and a midblock crosswalk. The team recorded count, thermal video, and DVR data during each trial. In addition, the team recorded ambient metadata—including ambient temperature, weather conditions (i.e., sunny, partly sunny, and cloudy), and wind speed—during data collection.

RESULTS

The research team calculated true detection accuracy, system accuracy, and F1 scores from the count data collected for each combination of factors and compared the data across the levels of each factor. The team used data from sensors C182, C183, and C184, All the intersection conditions included data from sensors C182 and C183; meanwhile, all the midblock conditions included data from sensor C184.

The research team could not assess the true detection accuracy and system accuracy of C181's count data because the count data from the sensors had not been recorded properly. Crossing B was on the fringes of the FOV for C181, and the detection zone went right to the edge of the sensor's FOV. As a result, the sensor could not detect when the vulnerable road user left the end of the detection zone, and the sensor aggregated no count data. Therefore, the team excluded all trials involving sensor C181 from this analysis. However, the team determined that C181 can detect vulnerable road users in all the scenarios because C181 still collected tracking data.

Table 6 shows the total number of vulnerable road user crossings, the total number of detections made by the sensors, the total number of times a sensors failed to successfully detect a vulnerable road user crossing, and the total number of times a sensor successfully detected a vulnerable road user crossing for each combination of factors. Using the count data, the research team calculated true detection accuracy, system accuracy, and F1 scores for each thermal sensor condition. Additionally, the team aggregated total crossings, detections, misses, and hits across all 56 conditions and calculated total true detection accuracy, system accuracy, and F1 score for the infrared thermal sensors.

Table 6. Infrared thermal imaging sensor outcomes and performance metrics by condition.

Vulnerable Road User Type	Location	Mode of Travel	Time of Day	Total Crossings	Total Detections	Total Misses	Total Hits	True Detection Accuracy (percent)	System Accuracy (percent)	F1 Score
Single adult pedestrian	Intersection	Fast	Day	12	11	3	9	75	82	0.78
Single adult pedestrian	Intersection	Fast	Night	12	12	0	12	100	100	1.00
Single adult pedestrian	Intersection	Slow	Day	12	13	1	11	92	85	0.88
Single adult pedestrian	Intersection	Slow	Night	11	11	0	11	100	100	1.00
Single adult pedestrian	Midblock	Fast	Day	6	3	3	3	50	100	0.67
Single adult pedestrian	Midblock	Fast	Night	6	6	0	6	100	100	1.00
Single adult pedestrian	Midblock	Slow	Day	6	4	2	4	67	100	0.80
Single adult pedestrian	Midblock	Slow	Night	6	6	0	6	100	100	1.00
Heavily clothed pedestrian	Intersection	Fast	Day	12	14	0	12	100	86	0.92
Heavily clothed pedestrian	Intersection	Fast	Night	12	12	0	12	100	100	1.00
Heavily clothed pedestrian	Intersection	Slow	Day	12	12	0	12	100	100	1.00
Heavily clothed pedestrian	Intersection	Slow	Night	12	13	0	12	100	92	0.96
Heavily clothed pedestrian	Midblock	Fast	Day	6	5	1	5	83	100	0.91
Heavily clothed pedestrian	Midblock	Fast	Night	6	6	0	6	100	100	1.00
Heavily clothed pedestrian	Midblock	Slow	Day	6	7	0	6	100	86	0.92
Heavily clothed pedestrian	Midblock	Slow	Night	6	6	0	6	100	100	1.00
Child pedestrian dummy	Intersection	Fast	Day	12	12	1	11	92	92	0.92
Child pedestrian dummy	Intersection	Fast	Night	12	12	0	12	100	100	1.00
Child pedestrian dummy	Intersection	Slow	Day	12	12	0	12	100	100	1.00
Child pedestrian dummy	Intersection	Slow	Night	12	12	0	12	100	100	1.00
Child pedestrian dummy	Midblock	Fast	Day	6	6	0	6	100	100	1.00
Child pedestrian dummy	Midblock	Fast	Night	6	6	0	6	100	100	1.00
Child pedestrian dummy	Midblock	Slow	Day	6	6	0	6	100	100	1.00
Child pedestrian dummy	Midblock	Slow	Night	6	6	0	6	100	100	1.00
Wheelchair user	Intersection	Fast	Day	12	12	0	12	100	100	1.00
Wheelchair user	Intersection	Fast	Night	12	12	0	12	100	100	1.00
Wheelchair user	Intersection	Slow	Day	12	11	1	11	92	100	0.96
Wheelchair user	Intersection	Slow	Night	12	12	0	12	100	100	1.00
Wheelchair user	Midblock	Fast	Day	6	5	1	5	83	100	0.91
Wheelchair user	Midblock	Fast	Night	6	6	0	6	100	100	1.00

Vulnerable Road User Type	Location	Mode of Travel	Time of Day	Total Crossings	Total Detections	Total Misses	Total Hits	True Detection Accuracy (percent)	System Accuracy (percent)	F1 Score
Wheelchair user	Midblock	Slow	Day	6	6	0	6	100	100	1.00
Wheelchair user	Midblock	Slow	Night	6	6	0	6	100	100	1.00
Three adult pedestrians	Intersection	Fast	Day	36	18	18	18	50	100	0.67
Three adult pedestrians	Intersection	Fast	Night	36	11	25	11	31	100	0.47
Three adult pedestrians	Intersection	Slow	Day	36	17	19	17	47	100	0.64
Three adult pedestrians	Intersection	Slow	Night	36	13	23	13	36	100	0.53
Three adult pedestrians	Midblock	Fast	Day	18	11	7	11	61	100	0.76
Three adult pedestrians	Midblock	Fast	Night	18	12	6	12	67	100	0.80
Three adult pedestrians	Midblock	Slow	Day	18	8	10	8	44	100	0.62
Three adult pedestrians	Midblock	Slow	Night	18	12	6	12	67	100	0.80
Bicyclist	Intersection	Fast	Day	12	12	0	12	100	100	1.00
Bicyclist	Intersection	Fast	Night	10	10	0	10	100	100	1.00
Bicyclist	Intersection	Slow	Day	12	12	0	12	100	100	1.00
Bicyclist	Intersection	Slow	Night	12	12	0	12	100	100	1.00
Bicyclist	Midblock	Fast	Day	6	6	0	6	100	100	1.00
Bicyclist	Midblock	Fast	Night	6	6	0	6	100	100	1.00
Bicyclist	Midblock	Slow	Day	6	5	1	5	83	100	0.91
Bicyclist	Midblock	Slow	Night	6	6	0	6	100	100	1.00
Scooter user	Intersection	Fast	Day	12	13	0	12	100	92	0.96
Scooter user	Intersection	Fast	Night	10	9	1	9	90	100	0.95
Scooter user	Intersection	Slow	Day	12	13	0	12	100	92	0.96
Scooter user	Intersection	Slow	Night	10	10	0	10	100	100	1.00
Scooter user	Midblock	Fast	Day	6	6	0	6	100	100	1.00
Scooter user	Midblock	Fast	Night	6	6	0	6	100	100	1.00
Scooter user	Midblock	Slow	Day	6	6	0	6	100	100	1.00
Scooter user	Midblock	Slow	Night	6	6	0	6	100	100	1.00
Total	—	—	—	641	523	129	512	79.88	97.90	0.88

—Not applicable.

The overall F1 score for the infrared thermal imaging sensors was 0.88 (acceptable). The majority of the conditions had F1 scores greater than 0.85. However, the three-adult-pedestrian conditions and most of the conditions with a single adult pedestrian during the day had unacceptable F1 scores.

The team then evaluated each factor independently of the other factors. Table 7 shows the performance metrics for each vulnerable-road-user condition in study 1, which evaluated the ability and applicability of infrared thermal imaging sensors.

Table 7. Performance of thermal sensors during study 1 for each vulnerable road user type.

Vulnerable Road User Type	True Detection Accuracy (percent)	System Accuracy (percent)	F1 Score
Single adult pedestrian	87.32	93.94	0.905
Heavily clothed pedestrian	98.61	94.67	0.966
Child pedestrian dummy	98.61	98.61	0.986
Wheelchair user	97.22	100.00	0.986
Three adult pedestrians	47.22	100.00	0.642
Bicyclist	98.57	100.00	0.993
Scooter user	98.53	97.10	0.978

Table 8 shows the performance of the thermal sensor at slow and fast speeds. Table 9 shows the performance of the thermal sensor at slow and fast speeds but excludes the three-adult-pedestrian conditions.

Table 8. Performance of thermal sensors during study 1 at slow and fast speeds.

Speed	True Detection Accuracy (percent)	System Accuracy (percent)	F1 Score
Slow	80.37	98.10	0.884
Fast	79.38	97.69	0.876

Table 9. Performance of thermal sensors during study 1 at slow and fast speeds without the three-adult-pedestrian conditions.

Speed	True Detection Accuracy (percent)	System Accuracy (percent)	F1 Score
Slow	97.65	97.65	0.977
Fast	95.28	97.12	0.962

Table 10 shows the performance of the thermal sensors during the day and at night. Table 11 shows the performance of the thermal sensors during the day and night but excludes the three-adult-pedestrian conditions.

Table 10. Performance of thermal sensors during study 1 during the day and night.

Time of Day	True Detection Accuracy (percent)	System Accuracy (percent)	F1 Score
Day	79.01	96.24	0.868
Night	80.76	99.61	0.892

Table 11. Performance metrics of thermal sensors during study 1 during the day and night without the three-adult-pedestrian conditions.

Time of Day	True Detection Accuracy (percent)	System Accuracy (percent)	F1 Score
Day	93.52	95.28	0.944
Night	99.52	99.52	0.995

Table 12 shows the performance of the thermal sensors at an intersection and at midblock. Table 13 shows the performance of the thermal sensors at an intersection and at midblock but excludes the three-adult-pedestrian conditions.

Table 12. Performance of thermal sensors during study 1 at an intersection and at midblock.

Location	True Detection Accuracy (percent)	System Accuracy (percent)	F1 Score
Intersection	78.35	97.08	0.867
Midblock	82.87	99.44	0.904

Table 13. Performance of thermal sensors during study 1 at an intersection and at midblock without the three-adult-pedestrian conditions.

Location	True Detection Accuracy (percent)	System Accuracy (percent)	F1 Score
Intersection	97.51	96.48	0.970
Midblock	94.44	99.27	0.968

CHAPTER 3. LIDAR SENSORS

This study investigated the ability and applicability of LiDAR sensors to provide accurate vulnerable road user volumetric data. The research team selected six different vulnerable road user types: a single pedestrian, a group of three pedestrians, a bicyclist, an electric scooter user, an electric wheelchair user, and a child pedestrian. The team observed these vulnerable road user types during the day in full daylight and at night under minimal lighting conditions. Additionally, the team assessed the vulnerable road user crossings at both an intersection crossing and a midblock crossing. Finally, the vulnerable road users crossed at both slow and high speeds for their types.

METHOD

Apparatus

The following 10 sections describe the technologies the research team used to conduct this study.

TFHRC Vulnerable Road User Technology Test Bed

The research team conducted testing on the TFHRC vulnerable road user technology test bed. The test bed comprises two marked, signalized intersections with pedestrian crosswalks; signal heads and call buttons; and one marked midblock crossing along a two-lane, two-way, 22-ft-wide road.

LiDAR Sensor

The research team selected one 32-channel LiDAR sensor located on the TFHRC vulnerable road user technology test bed intersection. This sensor had a measurement range of 650 ft, a range accuracy of ±3 cm, a 360° horizontal FOV, a 40° vertical FOV, and a frame rate of 5-20 Hz. The sensor had pedestrian and vehicle presence detection capabilities, vehicle and pedestrian counting, traffic data collection, traffic flow monitoring, and out-of-crosswalk occurrence detection. The research team set the sensor to detect and track the movements of pedestrians within its FOV.

The research team used proprietary software from the LiDAR sensor manufacturer to process and save the LiDAR sensor data and determine successful detection and counts. The software allowed for multimodal count data per a customizable counting zone definition. The research team visualized count data from specific locations and detection zones during designated periods using this software. The research team used these count data to verify detection of vulnerable road users and count data accuracy.

The sensor was set up along Innovation Drive, as shown in figure 5, which demonstrates the general locations of each sensor. The sensor was set up to observe both the intersection crosswalk and the midblock crosswalk within the TFHRC test bed. Each crosswalk was located within the OEM-determined FOV and detection distance of the sensor.

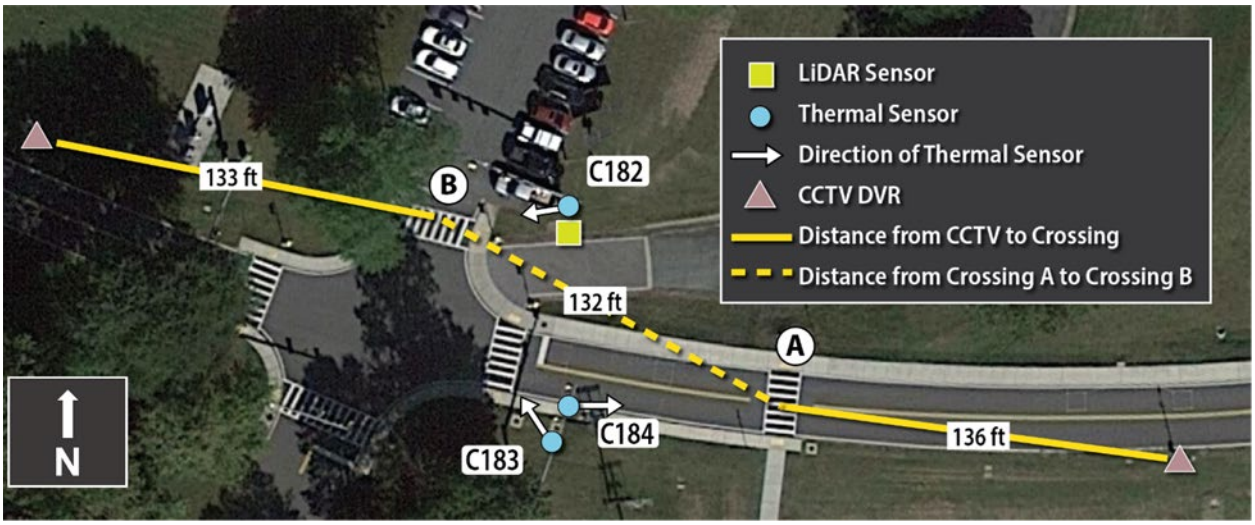

Original photo © 2023 Google® Earth™. Modified by FHWA (see Acknowledgments section).

Figure 5. Photo. Satellite image of TFHRC pedestrian technology test bed and location of LiDAR and thermal sensors.

LiDAR Sensor Roadside Data Processing Unit and Data Analytics Software

The research team processed the raw LiDAR data through a roadside data processing unit. The unit was installed at the intersection near the sensor and consisted of a 512-core graphics processing unit with 64 tensor cores; an 8-core, 64-bit central processing unit; and 32 gigabytes of 256-bit random access memory. The sensor was housed in milled aluminum housing. The roadside data processing unit allowed for edge-based computing, which enabled real-time data processing with the vendor's proprietary software license.

The proprietary data analytics software had several functionalities. The system aggregated count data for roadway agent detections every 15 minutes. To get and count individual crossings, the research team set the out-of-crosswalk event detection to include the crosswalk. From this process, the team was able to record and manually aggregate crosswalk crossings in the regions of interest.

CCTV DVRs

The research team used two traditional CCTV DVRs to record a live, high-resolution video feed in color during data collection. The CCTV DVRs were located 133 ft and 136 ft from the intersection and midblock crossings, respectively. The DVRs were zoomed in to clearly see vulnerable road user activity on the testing site. The video feed kept a record of the ground truth motion of vulnerable road users during testing. The video was then compared with the aggregate count output of the LiDAR sensors to verify the quality of the LiDAR sensor recording.

Video Recording Software

The research team used open-source video recording software coded to record data during trial runs of the CCTV DVRs. The team manually coded detections from video data when count data

failed to save properly, which happened in less than 3 percent of cases due to prematurely ending the saved count feed.

Electric Scooter

The study used a 350-W electric scooter with a 36-V, 15-Ah battery. Manufacturer documentation lists the scooter's top speed at 20 mph and load capacity as 220 lb.

Wheelchair

The study used an electric wheelchair with a 12-V battery. Manufacturer documentation lists the wheelchair's top speed at 4 mph and load capacity as 700 lb. The leg rests were attached and used during testing.

Bicycle

A research team member rode a 26-inch manual cruiser bicycle to represent bicyclists.

Belt-Driven Articulating Pedestrian Dummy

The team used a programmable articulating pedestrian dummy to simulate a child-size vulnerable road user. The child-size pedestrian dummy is 45.5 inches tall, roughly the average height of a 6-yr-old male child (Kuczmarski et al. 2000).

Vulnerable Road Users

The single adult pedestrian; the three adult pedestrians; and the operators of the wheelchair, scooter, and bicycle were members of the research team. The agents acting as these vulnerable road user types were a mix of males and females of various age ranges and races.

Experimental Design

Several unknowns regarding these sensors included their capabilities for midblock detection, differentiation, and identification of closely clustered pedestrians and their performance in adverse weather conditions. The selected LiDAR sensor was within the detection range defined by the OEM for either the designated intersection or the midblock crossing.

The research team conducted pilot testing for the sensors and setup. During piloting, the team tested each condition level of each factor at least twice to ensure no major issues with the LiDAR sensor setup or study design. The research team identified four key factors for the study: vulnerable road user type, speed, time of day, and location. Table 14 shows the condition levels for each factor. Study 1 established the specific values of each level of each factor to evaluate the ability of thermal imaging sensors (FHWA 2024). The only change for this aspect of the current study was using an electric wheelchair instead of a manual wheelchair and the exclusion of the heavy clothing condition.

Table 14. Factors and condition levels.

Factor	Condition Level
Vulnerable road user type	Single adult pedestrian Child-size pedestrian dummy Wheelchair user Three adult pedestrians Bicyclist Scooter user
Speed	Slow Fast
Time of day	Day Night
Location	Intersection Midblock

Vulnerable Road User Type

The research team chose six vulnerable road user types to evaluate the LiDAR sensors' ability to detect different vulnerable road users (table 14). Similar to study 1, the single-adult-pedestrian condition served as a comparison point for the performance of the other vulnerable road user types. The child pedestrian dummy simulated a child pedestrian, testing the LiDAR sensors' ability to detect vulnerable road users of different sizes. The advanced detection system was positioned so that the dummy could enter and leave the detection zone moving in one direction. The study used the condition with three adult pedestrians for determining the sensors' ability to detect multiple entities crossing in a group. In addition to those four pedestrian types, the three other levels included an adult wheelchair user, an adult bicyclist, and an adult scooter user. The adult-wheelchair-user condition operated a motorized electric wheelchair.

Speed

The research team established two levels of speed—slow and fast—for each vulnerable road user type. Table 15 outlines the speeds chosen for each vulnerable road user type. The principal investigator validated the speed from the live-tracking data during data collection.

Table 15. Fast and slow speeds for each vulnerable road user type.

Vulnerable Road User Type	Slow Speed (mph)	Fast Speed (mph)
Single adult pedestrian	2	5
Three adult pedestrians	2	5
Wheelchair user	2	5
Child-size pedestrian dummy	2	5
Bicyclist	5	10
Scooter user	5	10

Time of Day

The experiment used two levels—day and night—to test the sensors' ability to detect vulnerable road users under normal daylight conditions and at night when no ambient light existed. The research team defined day as any time during the period from at least 1 h after sunrise to 1 h before sundown of each day. The team defined night as any time during the period from at least 1 h after sundown to 1 h before sunrise. The definitions meant that researchers conducted experiments during the day time-of-day level in full daylight and experiments during the night time-of-day level when there was no light from the sun. Additionally, the research team collected ambient metadata, including weather (i.e., sunny, partly sunny, cloudy), although researchers did not collect data during very cloudy or adverse weather.

Location

The intersection and midblock crossings (figure 5) were chosen for data collection. These locations allowed road closing during testing to ensure team members' safety.

System Performance Metrics

The research team tested each of the 48 conditions 8 times. The team made a total of 384 observations. When collapsing the data across all factors except for vulnerable road user types, which had the largest number of levels, the total number of observations for each level was 64—an acceptable number of observations for a 95-percent confidence level (±5 percent). The total number of observations for the levels of the other factors was 192, an acceptable number of observations for a 95-percent confidence level (±5 percent).

This study's performance measures were true detection accuracy (recall), system accuracy (precision), and F1 score—a type of F score that measures accuracy by using precision and recall. Because both the recall and the precision of advanced detection technologies are important, an F1 score can be used. An F1 score measures accuracy and incorporates the proportion of hits compared with all trials (including misses) and all detections (including false positives), weighing those two aspects of accuracy equally.

Table 16 lists the four potential outcomes for any single trial (i.e., detection or no detection) that occurred during data collection. Agencies use these potential outcomes to calculate the established performance metrics. True detection accuracy measures the LiDAR sensors' ability to detect vulnerable road users while also accounting for misses. For example, if the sensor makes 5 successful detections out of 10 possible correct detections, the true detection accuracy rate is 50 percent. System accuracy measures the LiDAR sensors' ability to detect only vulnerable road users and exclude nonvulnerable road users and false detections. For example, if the sensor makes a total of 10 detections but only 8 were accurate detections of actual vulnerable road users (i.e., 2 false detections), the system accuracy rate is 80 percent.

Table 16. Potential outcomes for a single trial of data collection.

Vulnerable Road User Crossing	Sensor Output	Outcome
Crossing	Detection	Hit
Crossing	No detection	Miss
No crossing	Detection	False detection
No crossing	No detection	Correct rejection

The research team used true detection accuracy as a measure to determine the abilities of the sensors. The team used system accuracy in conjunction with true detection accuracy to calculate an F1 score. The team used the F1 score to assess the applicability of the LiDAR sensors for detecting vulnerable road users. Applicability of the sensors is based on their ability to not only detect vulnerable road users but also to minimize false detections.

Figure 6 through figure 8 show equations for the chosen performance metrics.

$$\sum Hits/\left(\sum Hits + \sum Misses\right)$$

Figure 6. Equation. True detection accuracy.

$$\sum Hits/\left(\sum Hits + \sum False\ Detections\right)$$

Figure 7. Equation. System accuracy.

$$2\frac{(True\ detection\ accuracy * System\ accuracy)}{(True\ detection\ accuracy + System\ accuracy)}$$

Figure 8. Equation. F1 score.

The higher the value of true detection accuracy, the more likely the system can detect vulnerable road users when a vulnerable road user is truly present. Based on El-Urfali et al. (2019), the team set the minimum acceptable F1 score as 0.85 and the minimum acceptable true detection accuracy as 85 percent. Any scores less than those scores resulted in unacceptable performance (table 17).

Table 17. True detection accuracy thresholds.

F1 Score	True Detection Accuracy (percent)	Rating
≥0.85	≥85	Acceptable performance
≤0.84	≤84	Unacceptable performance

DATA ANALYSIS AND RESULTS

The research team calculated true detection accuracy, system accuracy, and F1 scores from the count data collected for each combination of factors and compared the data across the levels of each factor. The team used data from sensor C284 to collect all the intersection and midblock conditions. Table 18 shows the total number of vulnerable road user crossings (total number of hits and misses), total detections (hits and false positives), total number of misses, and total number of hits for each combination of factors. Using the count data, the research team calculated true detection accuracy, system accuracy, and F1 scores for each condition of the LiDAR sensors. The team aggregated total crossings, detections, misses, and hits across all 56 conditions and calculated total true detection accuracy, system accuracy, and F1 score for the LiDAR sensors. Some values under system accuracy and F1 score are listed as not applicable because these trials had no hits or false positives, thus resulting in 0 being divided by 0, a nonapplicable value.

Table 18. LiDAR sensor outcomes and performance metrics by condition.

Vulnerable Road User Type	Location	Mode of Travel	Time of Day	Total Crossings	Total Detections	Total Misses	Total Hits	True Detection Accuracy (percent)	System Accuracy (percent)	F1 Score
Single adult pedestrian	Intersection	Fast	Day	8	8	0	8	100	100	1.00
Single adult pedestrian	Intersection	Fast	Night	8	8	0	8	100	100	1.00
Single adult pedestrian	Intersection	Slow	Day	8	8	0	8	100	100	1.00
Single adult pedestrian	Intersection	Slow	Night	8	8	0	8	100	100	1.00
Single adult pedestrian	Midblock	Fast	Day	8	8	0	8	100	100	1.00
Single adult pedestrian	Midblock	Fast	Night	8	8	0	8	100	100	1.00
Single adult pedestrian	Midblock	Slow	Day	8	8	0	8	100	100	1.00
Single adult pedestrian	Midblock	Slow	Night	8	8	0	8	100	100	1.00
Child pedestrian dummy	Intersection	Fast	Day	8	0	8	0	0	—	—
Child pedestrian dummy	Intersection	Fast	Night	8	0	8	0	0	—	—
Child pedestrian dummy	Intersection	Slow	Day	8	0	8	0	0	—	—
Child pedestrian dummy	Intersection	Slow	Night	8	0	8	0	0	—	—
Child pedestrian dummy	Midblock	Fast	Day	8	0	8	0	0	—	—
Child pedestrian dummy	Midblock	Fast	Night	8	0	8	0	0	—	—
Child pedestrian dummy	Midblock	Slow	Day	8	0	8	0	0	—	—
Child pedestrian dummy	Midblock	Slow	Night	8	0	8	0	0	—	—
Wheelchair user	Intersection	Fast	Day	8	5	3	5	62	100	0.77
Wheelchair user	Intersection	Fast	Night	8	7	1	7	88	100	0.93
Wheelchair user	Intersection	Slow	Day	8	0	8	0	0	—	—

Vulnerable Road User Type	Location	Mode of Travel	Time of Day	Total Crossings	Total Detections	Total Misses	Total Hits	True Detection Accuracy (percent)	System Accuracy (percent)	F1 Score
Wheelchair user	Intersection	Slow	Night	8	0	8	0	0	—	—
Wheelchair user	Midblock	Fast	Day	8	7	1	7	88	100	0.93
Wheelchair user	Midblock	Fast	Night	8	7	1	7	88	100	0.93
Wheelchair user	Midblock	Slow	Day	8	8	0	8	100	100	1.00
Wheelchair user	Midblock	Slow	Night	8	8	0	8	100	100	1.00
Three adult pedestrians	Intersection	Fast	Day	24	8	16	8	33	100	0.50
Three adult pedestrians	Intersection	Fast	Night	24	5	19	5	21	100	0.34
Three adult pedestrians	Intersection	Slow	Day	24	8	16	17	33	100	0.50
Three adult pedestrians	Intersection	Slow	Night	24	6	18	6	25	100	0.40
Three adult pedestrians	Midblock	Fast	Day	24	9	15	9	38	100	0.55
Three adult pedestrians	Midblock	Fast	Night	24	8	16	8	33	100	0.50
Three adult pedestrians	Midblock	Slow	Day	24	12	12	12	50	100	0.67
Three adult pedestrians	Midblock	Slow	Night	24	7	17	7	29	100	0.45
Bicyclist	Intersection	Fast	Day	8	1	7	1	12	100	0.22
Bicyclist	Intersection	Fast	Night	8	0	8	0	—	—	—
Bicyclist	Intersection	Slow	Day	8	6	2	6	75	100	0.86
Bicyclist	Intersection	Slow	Night	8	6	2	6	75	100	0.86
Bicyclist	Midblock	Fast	Day	8	6	2	6	75	100	0.86
Bicyclist	Midblock	Fast	Night	8	5	3	5	62	100	0.77
Bicyclist	Midblock	Slow	Day	8	7	1	7	88	100	0.93

Vulnerable Road User Type	Location	Mode of Travel	Time of Day	Total Crossings	Total Detections	Total Misses	Total Hits	True Detection Accuracy (percent)	System Accuracy (percent)	F1 Score
Bicyclist	Midblock	Slow	Night	8	6	2	6	75	100	0.86
Scooter user	Intersection	Fast	Day	8	2	6	2	25	100	0.40
Scooter user	Intersection	Fast	Night	8	0	8	0	—	—	—
Scooter user	Intersection	Slow	Day	8	4	4	4	50	100	0.67
Scooter user	Intersection	Slow	Night	8	8	0	8	100	100	1.00
Scooter user	Midblock	Fast	Day	8	0	8	0	—	—	—
Scooter user	Midblock	Fast	Night	8	0	8	0	—	—	—
Scooter user	Midblock	Slow	Day	8	7	1	7	88	100	0.93
Scooter user	Midblock	Slow	Night	8	6	2	6	75	100	0.86

—Not applicable.

Study 2 evaluated LiDAR sensors in isolation and subsequently compared the two sensor types. The overall true detection accuracy for the LiDAR sensors was 79.88 percent, suggesting overall unacceptable performance (i.e., less than 85 percent). Most of the conditions had true detection accuracy less than 85 percent. However, the single adult pedestrian had 100-percent true detection accuracy under all conditions. The team evaluated each factor independently of the other factors. Table 19 shows the performance metrics of the LiDAR sensors for each vulnerable road user condition.

Table 19. Performance of LiDAR sensors across vulnerable road user types.

Vulnerable Road User Type	True Detection Accuracy (percent)	System Accuracy (percent)	F1 Score
Single adult pedestrian	100	100	1.00
Child pedestrian dummy	0	—	—
Wheelchair user	66	100	0.79
Three adult pedestrians	33	100	0.49
Bicyclist	57.9	100	0.73
Scooter user	42	100	0.59
Overall	79.88	100	0.89

—Not applicable.

Table 20 shows the performance of the LiDAR sensor at slow and fast speeds. Table 21 shows the performance of the LiDAR sensor at slow and fast speeds, excluding the three-adult-pedestrian conditions.

Table 20. Performance of LiDAR sensors at slow and fast speeds.

Speed	True Detection Accuracy (percent)	System Accuracy (percent)	F1 Score
Slow	51	100	0.68
Fast	40	100	0.57

Table 21. Performance of LiDAR sensors at slow and fast speeds (excluding three-adult-pedestrian condition).

Speed	True Detection Accuracy (percent)	System Accuracy (percent)	F1 Score
Slow	61	100	0.76
Fast	45	100	0.62

Table 22 shows the performance of the LiDAR sensors during the day and night conditions. Table 23 shows the performance of the LiDAR sensors during the day and night, excluding the three-adult-pedestrian conditions.

Table 22. Performance of LiDAR sensors during day and night.

Time of Day	True Detection Accuracy (percent)	System Accuracy (percent)	F1 Score
Day	48	100	0.65
Night	43	100	0.60

Table 23. Performance metrics of LiDAR sensors during day and night (excluding the three-adult-pedestrian condition).

Time of Day	True Detection Accuracy (percent)	System Accuracy (percent)	F1 Score
Day	53	100	0.69
Night	53	100	0.69

Table 24 shows the performance of the LiDAR sensors at an intersection and at midblock. Table 25 shows the performance of the LiDAR sensors at an intersection and at midblock, excluding the three-adult-pedestrian conditions.

Table 24. Performance of LiDAR sensors at an intersection and at midblock.

Location	True Detection Accuracy (percent)	System Accuracy (percent)	F1 Score
Intersection	38	100	0.55
Midblock	53	100	0.69

Table 25. Performance of LiDAR sensors at an intersection and at midblock (excluding three-adult-pedestrian condition).

Location	True Detection Accuracy (percent)	System Accuracy (percent)	F1 Score
Intersection	44	100	0.61
Midblock	62	100	0.76

CHAPTER 4. GENERAL DISCUSSION AND SENSOR COMPARISON

In the first study, which investigated the infrared thermal sensors, researchers found that infrared thermal imaging sensors have many advantages for vulnerable road user detection. These sensors were able to detect different vulnerable road user types (pedestrians, bicyclists, scooter users, and wheelchair users), vulnerable road users traveling at fast and slow speeds, vulnerable road users during the day and at night, and vulnerable road users at both intersections and midblock crossings. One of the greatest advantages of the infrared thermal imaging sensors is their ability to detect vulnerable road users at night, when visibility is poor. These sensors were unable to differentiate between and categorize the different vulnerable road users but could potentially improve overall count data for individual vulnerable road users on roadways, serving to better measure vulnerable road user exposure to crash risk.

Another major disadvantage of the thermal sensors was their inability to detect three pedestrians crossing in a closely clustered triangular formation. The inability of the sensors to successfully detect multiple, closely clustered vulnerable road users can potentially lead to lower overall counts of vulnerable road users and make exposure to crash risk seem higher than it actually is. Considering that FHWA's (2016) *Traffic Monitoring Guide* states that pedestrians often cross roadways in closely spaced groups, that inability is a significant disadvantage.

In the second study, which included assessing the ability of LiDAR sensors, researchers found the LiDAR sensors, when used in conjunction with the roadside data processing unit and analytics software, had both advantages and disadvantages in detecting vulnerable road users. Specifically, the LiDAR sensors were able to detect the single adult pedestrian type very well. However, other vulnerable road user types were either not detected at all (e.g., child pedestrian dummy) or only detected sometimes. Whether the vulnerable road users were crossing during the day or at night did not make a difference in the detection outcome, as no consistent patterns were observed—suggesting that the sensors work equally well during the day and night. However, the sensors displayed differences in their abilities to detect certain vulnerable road user types. The inability of these sensors to differentiate between pedestrians, bicyclists, scooter users, and wheelchair users was a disadvantage.

The detection algorithm and the data libraries need further development so that sensors not only detect but also define the different types of vulnerable road users. However, the sensors have the potential to improve overall count data for individual vulnerable road users on the roadways, which can potentially serve to better measure vulnerable road user exposure to crash risk. The sensors could not accurately detect three pedestrians crossing in a closely clustered triangular formation, and this inability can potentially lead to lower overall counts of vulnerable road users and makes crash risk exposure seem higher than it is. Because pedestrians often cross roadways in closely spaced groups, this inability is a major disadvantage (FHWA 2016).

During the LiDAR study, the research team collected a second round of thermal sensor data, making comparisons possible of the performance (true detection accuracy and F1 scores) of not only the LiDAR and thermal sensors from the second study's data collection but also the performance of the thermal sensors across two separate time points. The Analysis section that follows provides performance metrics for the second round of thermal sensor data collection, a

comparison of the performance of the two rounds of thermal data collection, and a comparison of the LiDAR sensors and thermal sensors.

ANALYSIS

Infrared Thermal Sensor Data From Study 2

Table 26 shows the performance of the thermal sensors for each vulnerable road user type. Table 27 shows sensor performance at slow and fast speeds. Table 28 shows the performance of the thermal sensors at slow and fast speeds but excludes the three-adult-pedestrian conditions.

Table 26. Performance of thermal sensors during study 2 across vulnerable road user types.

Vulnerable Road User Type	True Detection Accuracy (percent)	System Accuracy (percent)	F1 Score
Single adult pedestrian	84	91	0.88
Child pedestrian dummy	88	98	0.92
Wheelchair user	91	99	0.95
Three adult pedestrians	38	100	0.55
Bicyclist	89	96	0.92
Scooter user	83	91	0.87

Table 27. Performance of thermal sensors during study 2 at slow and fast speeds.

Speed	True Detection Accuracy (percent)	System Accuracy (percent)	F1 Score
Slow	65	95	0.77
Fast	72	97	0.83

Table 28. Performance of thermal sensors during study 2 at slow and fast speeds without three-adult-pedestrian conditions.

Speed	True Detection Accuracy (percent)	System Accuracy (percent)	F1 Score
Slow	85	94	0.89
Fast	89	96	0.92

Table 29 shows the performance of the thermal sensors during the day and at night. Table 30 shows the performance of the thermal sensors during the day and night but excludes the three-adult-pedestrian conditions.

Table 29. Performance of thermal sensors during study 2 during the day and night.

Time of Day	True Detection Accuracy (percent)	System Accuracy (percent)	F1 Score
Day	71	96	0.81
Night	67	96	0.79

Table 30. Performance metrics of thermal sensors during study 2 during the day and night without the three-adult-pedestrian conditions.

Time of Day	True Detection Accuracy (percent)	System Accuracy (percent)	F1 Score
Day	84	94	0.89
Night	90	95	0.92

Table 31 shows the performance of the thermal sensors at an intersection and at midblock. Table 32 shows the performance of the thermal sensors at an intersection and at midblock but excludes the three-adult-pedestrian conditions.

Table 31. Performance of thermal sensors during study 2 at an intersection and at midblock.

Location	True Detection Accuracy (percent)	System Accuracy (percent)	F1 Score
Intersection	69	95	0.8
Midblock	67	98	0.8

Table 32. Performance of thermal sensors during study 2 at an intersection and at midblock without the three-adult-pedestrian conditions.

Location	True Detection Accuracy (percent)	System Accuracy (percent)	F1 Score
Intersection	88	94	0.91
Midblock	85	97	0.91

Notably, the data collection for the thermal sensors during study 2 was slightly different than the first round of data collection. Specifically, researchers conducted eight trials for each condition, compared to the six conducted in study 1. Additionally, the researchers excluded the heavy clothing condition from study 2. Researchers included the heavy clothing condition in study 1 to see if the insulation from the heavy clothing would impair the thermal sensors' ability to detect pedestrians. Based on the results from study 1, the researchers deemed that insulation did not have an effect on the thermal sensors' ability and would not influence the ability of the LiDAR sensors. Therefore, this condition was excluded from the comparison. Finally, a motorized wheelchair was used in study 2 in place of the manual wheelchair used in study 1.

Comparison of Thermal Sensor Performance Across Study 1 and 2

The following results are based on a Poisson regression model of the two sets of data collected from the thermal sensors across the intersection and midblock using true detection accuracy, system accuracy, and the F1 score as dependent variables.

Table 33 shows study 2 had lower true detection accuracy compared with study 1. The analysis indicated the thermal sensors were less likely to detect vulnerable road users crossing at an intersection in study 2, as compared with study 1 ($p = 0.003$). When the thermal sensors detected a crossing in both studies, the likelihood that the crossing was a true event was high. Study 2 had a lower F1 score compared with study 1 because study 2 also had lower true detection accuracy.

Table 33. Performance of thermal sensors from study 1 and study 2 at intersection with the three-adult-pedestrian conditions (excluding heavy clothing condition).

Experiment	True Detection Accuracy (percent)	System Accuracy (percent)	F1 Score
1	76	98	0.86
2	69	95	0.8

Table 34 shows that study 2 had lower true detection accuracy than study 1. The analysis indicated thermal sensors from study 2 were less likely to detect vulnerable road users, excluding the three adult vulnerable road user conditions , as compared with study 1 ($p = 0.0003$). When thermal sensors detected a crossing in both experiments, the likelihood that a crossing was a true event was high. Study 2 had a lower F1 score than study 1 because of study 2's lower true detection accuracy.

Table 34. Performance of thermal sensors from study 1 and study 2 at intersection without the three-adult-pedestrian conditions (excluding heavy clothing condition).

Experiment	True Detection Accuracy (percent)	System Accuracy (percent)	F1 Score
1	97	97	0.97
2	88	94	0.91

Table 35 shows that study 2 had lower true detection accuracy at midblock crossings than study 1. The analysis indicated the thermal sensors from study 2 were less likely to detect vulnerable road users at midblock crossings, as compared with the first experiment ($p = 0.003$). When the thermal sensors detected a crossing in both study 1 and study 2, the likelihood that the crossing was a true event was nearly perfect. Study 2 had a lower F1 score than study 1 because of study 2's lower true detection accuracy.

Table 35. Performance of thermal sensors from study 1 and study 2 at midblock with the three-adult-pedestrian conditions (excluding heavy clothing condition).

Experiment	True Detection Accuracy (percent)	System Accuracy (percent)	F1 Score
1	81	100	0.9
2	67	98	0.8

Table 36 shows that study 2 had lower true detection accuracy than study 1 at midblock crossings, excluding the three adult pedestrian conditions. The analysis indicated the thermal sensors from study 2 were less likely to detect vulnerable road users at a midblock crossing, excluding the three adult pedestrian conditions, as compared with study 1 ($p = 0.02$). When the thermal sensor detected a crossing in study 1 and study 2, the likelihood that the crossing was a true event was nearly perfect. Study 2 had a lower F1 score than study 1 because of study 2's lower true detection accuracy.

Table 36. Performance of thermal sensors from study 1 and study 2 at midblock without the three-adult-pedestrian conditions (excluding heavy clothing condition).

Experiment	True Detection Accuracy (percent)	System Accuracy (percent)	F1 Score
1	94	100	0.97
2	85	97	0.91

Comparison of Thermal and LiDAR Sensor Performance

The research team used a Poisson regression model to compare the true detection accuracy, system accuracy, and F1 score of the thermal sensors and LiDAR sensors at both the intersection and midblock. The child dummy, scooter, wheelchair, and bike-night-fast-speed conditions were all excluded because the LiDAR sensors were unable to make any detections of those vulnerable road user types under certain conditions. Only conditions in which at least one detection was successfully made for all conditions were included.

Table 37 shows the LiDAR sensor had lower true detection accuracy than the thermal sensor at the intersection crossing, although the analysis did not show a significant difference between LiDAR and thermal sensors in capturing a crossing. When both sensors detected a crossing, the likelihood that the crossing was a true event was nearly perfect. The LiDAR sensors had a lower F1 score than the thermal sensors because of the LiDAR sensor's lower true detection accuracy.

Table 37. Performance of LiDAR and thermal sensors at intersection with the three-adult-pedestrian conditions (excluding child dummy, scooter, and wheelchair conditions and all fast bicycle night trails).

Sensor	True Detection Accuracy (percent)	System Accuracy (percent)	F1 Score
Thermal	56	97	0.71
LiDAR	47	100	0.64

Table 38 shows the LiDAR sensor had lower true detection accuracy than the thermal sensor at the intersection even when excluding the three adult pedestrian conditions. The analysis indicated the LiDAR sensor was less likely to capture a crossing, as compared with the thermal sensor ($p = 0.04$). When both sensors detected a crossing, the likelihood that the crossing was a true event was high. The LiDAR sensor had a lower F1 score than the thermal sensor because of the LiDAR sensor's lower true detection accuracy.

Table 38. Performance of LiDAR and thermal sensors at intersection without the three-adult-pedestrian conditions (excluding child dummy, scooter, and wheelchair conditions and all fast bicycle night trails).

Sensor	True Detection Accuracy (percent)	System Accuracy (percent)	F1 Score
Thermal	95	95	0.95
LiDAR	80	100	0.89

Table 39 shows the LiDAR sensor had higher true detection accuracy than the thermal sensor at the midblock crossing, although the analysis did not show a significant difference between the LiDAR and thermal sensors in capturing a crossing. When both sensors detected a crossing, the likelihood that the crossing was a true event was nearly perfect. The thermal sensor had a lower F1 score than the LiDAR sensor because of the thermal sensor's lower true detection accuracy.

Table 39. Performance of LiDAR and thermal sensors at midblock with the three-adult-pedestrian conditions (excluding child dummy and scooter conditions.)

Sensor	True Detection Accuracy (percent)	System Accuracy (percent)	F1 Score
Thermal	61	97	0.75
LiDAR	64	100	0.78

Table 40 shows the LiDAR sensor had higher true detection accuracy than the thermal sensor at the midblock crossing even when excluding the three adult pedestrians conditions, but the analysis didn't show a significant difference in the likelihood of capturing a crossing between the LiDAR and thermal sensors. When both sensors detected a crossing, the likelihood that the crossing was a true event was high. The thermal sensor had a lower F1 score than the LiDAR sensor because of the thermal sensor's lower true detection accuracy.

Table 40. Performance of LiDAR and thermal sensors at midblock without the three-adult-pedestrian conditions (excluding child dummy and scooter conditions.)

Sensor	True Detection Accuracy (percent)	System Accuracy (percent)	F1 Score
Thermal	84	95	0.89
LiDAR	90	100	0.95

DISCUSSION AND CONCLUSION

Based on the results of the comparison, the performance of the thermal sensors across the first and second rounds of data collection differed significantly. Specifically, the sensors had better true-detection accuracy in the first round of data collection compared with the second round at both the midblock and intersection crossings. No statistical difference was present between system accuracy scores for study 1 and study 2. F1 scores were significantly different but only due to the difference in the true detection accuracy of the two time points.

These types of advanced detection technologies must have the ability to consistently detect vulnerable road users in real-world settings to improve the collection of vulnerable road user volumetric data. As such, the inconsistency in thermal sensor performance between study 1 and study 2 suggests the thermal sensors used in this study may not improve real-world vulnerable road user volumetric data—and thus are not suitable for real-world application.

Several possible explanations exist for the significant differences in performance of the thermal sensors between study 1 and study 2 , as follows:

- Study 2 had more trials. If study 1 also had more trials, the sensor detection rates of study 1 might have been closer to the detection rates of study 2. If a larger sample size, based on a different power analysis, is collected in future studies, the differences may possibly disappear.

- Study 1 used a manual wheelchair, but study 2 used an electric-powered wheelchair. When comparing the true detection accuracies of the different vulnerable road user types, a difference existed between the detection of wheelchair users in study 1 compared to Study 2 (97 percent to 91 percent, respectively). However, this reduction in true detection accuracy can also be seen in all the other vulnerable road user types—suggesting the difference in the types of wheelchairs wasn't the only possible explanation for the sensor performance differences during the two rounds.

- Study 1 took place from January to April, and study 2 took place from September to December. However, the difference in average temperature across the data collection periods was only 2 °F (61.30 °F versus 59.34 °F, respectively).

Regardless of the inconsistency in the performance of the thermal sensors, a greater difference occurred between the thermal and LiDAR sensors. Overall, the thermal sensors performed better than the LiDAR sensors at the intersection, but the LiDAR sensors performed better at the midblock crossing, whether including or excluding the three-adult-pedestrian trials. Notably, however, several conditions were excluded from this comparison due to the LiDAR's inability to make any detections. Specifically, the LiDAR was unable to detect most conditions involving the vulnerable road user types that used a scooter or a wheelchair and the bicyclist traveling fast at night. It was also unable to make a single detection of the child pedestrian dummy. The fact that the LiDAR was unable to detect any trials of these specific vulnerable road user types is a significant weakness when compared to the performance of the thermal sensors.

Overall, the LiDAR sensor failed to meet most of the criteria needed for the sensor to be applicable for real-world use; meanwhile, the thermal sensor, despite being slightly inconsistent in its detection rates, met far more of the criteria. However, both sensors were not able to detect multiple pedestrians clustered closely together, which is primarily how pedestrians cross through crosswalks in highly populated areas. Additional developments and advancements of these sensors and the data processing software and detection algorithms must be made before these sensors can consistently improve the detection rates of vulnerable road users in active roadways.

That said, technology evolves at a rapid pace; as such, the sensors used in these studies are already outdated. The LiDAR sensors used are no longer in distribution, and a new version of the infrared thermal imaging sensors uses updated detection technology integrated into the sensors. The new LiDAR sensors would presumably have a greater number of lasers and thus a denser point cloud, allowing for more detail in detecting agents in the roadway. Furthermore, since the beginning of the current project, the infrared thermal imaging sensors are reputed to have a new processing algorithm with an improved method for detecting and classifying agents on the roadway.

Considering these study results and the rapid growth of detection technologies, these technologies, such as thermal and LiDAR sensors (with enough time and development from manufacturers) may one day be used to improve vulnerable road user detection, consequently improving the collection of vulnerable road user volumetric data on real-world roads. This volumetric data will be crucial in helping researchers determine the true level of exposure vulnerable road users face when crossing our roadways, both at intersections and at midblock crossings.

ACKNOWLEDGEMENTS

The original maps for figure 1 and figure 5 are the copyright property of Google® Earth™ and can be accessed from https://www.google.com/earth (Google 2024). FHWA modified the maps to note locations of sensors, crosswalk labels, and distances.

REFERENCES

American National Standards Institute. 2007. *Manual on Classification of Motor Vehicle Traffic Accidents*, 7th edition. ANSI D16.1-2007. Itasca, IL: National Safety Council.

Ansariyar, A., and M. Jeihani. 2023. "Investigating the Vehicle-Bicyclists Conflicts Using LIDAR Sensor Technology at Signalized Intersections." Presented at the *ICTTE 2023: International Conference on Transportation and Traffic Engineering*. Wuhan, China: Wuhan University of Technology. https://papers.ssrn.com/sol3/papers.cfm?abstract_id=4473399, last accessed August 14, 2024.

El-Urfali, A., L. Pei-Sung, A. Kourtellis, Z. Wang, and C. Chen. 2019. *Integration of a Robust Automated Pedestrian Detection System for Signalized Intersections: Final Report*. Tallahassee, FL: Florida Department of Transportation. https://rosap.ntl.bts.gov/view/dot/64442/dot_64442_DS1.pdf, last accessed August 14, 2024.

FHWA. n.d. "Enhancing Vulnerable Road User Detection and Volume Data Through Advanced Imaging Techniques" (web page). https://highways.dot.gov/research/projects/enhancing-vulnerable-road-user-detection-and-volume-data-through-advanced-imaging, last accessed September 19, 2024.

FHWA. 2016. *Traffic Monitoring Guide*. Report No. FHWA-PL-17-003. Washington, DC: Federal Highway Administration. https://www.fhwa.dot.gov/policyinformation/tmguide/tmg_fhwa_pl_17_003.pdf, last accessed August 14, 2024.

FHWA. 2024. *TechBrief: Enhancing Vulnerable Road User Detection and Volume Data Through the Use of Infrared Thermal Imaging Sensors*. Publication No. FHWA-HRT-24-135. https://highways.dot.gov/sites/fhwa.dot.gov/files/FHWA-HRT-24-135.pdf, last accessed August 14, 2024.

Google. 2024. "Google® Earth™" (web page). https://www.google.com/earth, last accessed August 16, 2024.

GPO. 2024a. "Vulnerable Road User." U.S.C. 23 §148(a)(15). 2024. https://uscode.house.gov/view.xhtml?req=granuleid:USC-prelim-title23-section148&num=0&edition=prelim#amendment-note, last accessed October 9, 2024.

GPO. 2024b. "Definitions." 23 CFR 924.3 §490.205. https://www.govinfo.gov/app/details/CFR-2024-title23-vol1/CFR-2024-title23-vol1-sec490-205, last accessed October 2, 2024.

Jannat, M., S. M. Roldan, S. A. Balk, and K. Timpone. 2021. "Assessing Potential Safety Benefits of Advanced Pedestrian Technologies Through a Pedestrian Technology Test Bed." *Journal of Intelligent Transportation Systems* 25, no. 2: 139–156. https://www.tandfonline.com/doi/full/10.1080/15472450.2020.1807347, last accessed August 14, 2024.

Ismail, K., T. Sayed, N. Saunier, and C. Lim. 2009. "Automated Analysis of Pedestrian–Vehicle Conflicts Using Video Data." *Transportation Research Record* 2140, no. 1: 44–54. https://journals.sagepub.com/doi/10.3141/2140-05, last accessed August 14, 2024.

Khaled, A., O. Shalash, and O. Ismaeil. 2023. "Multiple Objects Detection and Localization Using Data Fusion." Presented at the 2023 *2nd International Conference on Automation, Robotics, and Computer Engineering (ICARCE)*. Wuhan, China: Institute of Electrical and Electronics Engineers. https://ieeexplore.ieee.org/document/10492609, last accessed August 14, 2024.

Kuczmarski, R. J., C. L. Ogden, L. M. Grummer-Strawn, and K. Flegal, et al. 2000. "CDC Growth Charts: United States." *Advance Data From Vital and Health Statistics* 314: 1-27. https://www.cdc.gov/nchs/data/ad/ad314.pdf, last accessed August 14, 2024.

Liu, Y., H. Su, C. Zeng, and X. Li. 2021. "A Robust Thermal Infrared Vehicle and Pedestrian Detection Method in Complex Scenes." *Sensors* 21, no. 4: 1240. https://www.mdpi.com/1424-8220/21/4/1240, last accessed August 14, 2024.

Lv, B., R. Sun, H. Zhang, H. Xu, and R. Yue. 2019. "Automatic Vehicle-Pedestrian Conflict Identification With Trajectories of Road Users Extracted From Roadside LiDAR Sensors Using a Rule-Based Method." *IEEE Access* 7: 161594–161606. https://ieeexplore.ieee.org/document/8892489, last accessed August 14, 2024.

NCSA. 2024a. *Traffic Safety Facts 2022 Data: Bicyclists and Other Cyclists*. Report No. DOT HS 813 591. Washington, DC: National Highway Traffic Safety Administration. https://crashstats.nhtsa.dot.gov/Api/Public/Publication/813591, last accessed August 14, 2024.

NCSA. 2024b. *Traffic Safety Facts 2022 Data: Pedestrians.* Report No. DOT HS 813 590. Washington, DC: National Highway Traffic Safety Administration. https://crashstats.nhtsa.dot.gov/Api/Public/Publication/813590, last accessed August 14, 2024.

North American Bikeshare and Scootershare Association. 2022. *3rd Annual Shared Micromobility State of the Industry Report*. Portland, ME: North American Bikeshare and Scootershare Association.

Organisation for Economic Co-operation and Development. 1998. *Safety of Vulnerable Road Users*. Publication No. IRRD 895623. Paris, France: Organisation for Economic Co-operation and Development.

Reyes-Muñoz, A., and J. Guerrero-Ibáñez. 2022. "Vulnerable Road Users and Connected Autonomous Vehicles Interaction: A Survey." *Sensors* 22, no. 12. https://doi.org/10.3390/s22124614,

Rothman, L., A. W. Howard, A. Camden, and C. Macarthur. 2012. "Pedestrian Crossing Location Influences Injury Severity in Urban Areas." *Injury Prevention* 18, no. 6: 365-370. https://www.doi.org/10.1136/injuryprev-2011-040246, last accessed August 14, 2024.

Ryus, P., E. Ferguson, K. M. Laustsen, R. J. Schneider, F. R. Proulx, T. Hull, and L. Miranda-Moreno. 2014. *NCHRP Report 797: Guidebook on Pedestrian and Bicycle Volume Data Collection*. Washington, DC: The National Academies Press.

Teixeira, P., S. Sargento, P. Rito, M. Luís, and F. Castro. 2023. "A Sensing, Communication and Computing Approach for Vulnerable Road Users Safety." *IEEE Access* 11: 4914–4930. https://ieeexplore.ieee.org/document/10013676, last accessed August 14, 2024.

Vargas, J., S. Alsweiss, O. Toker, R. Razdan, and J. Santos. 2021. "An Overview of Autonomous Vehicles Sensors and Their Vulnerability to Weather Conditions." *Sensors* 21, no. 16. https://www.mdpi.com/1424-8220/21/16/5397, last accessed August 14, 2024.

Walker, C. J. 2022. Cheryl J. Walker to Division Administrators, memorandum, October 21, 2022. "Action: Vulnerable Road User Safety Assessment Guidance (Due date: November 15 2023)." https://highways.dot.gov/sites/fhwa.dot.gov/files/2022-10/VRU%20Safety%20Assessment%20Guidance%20FINAL_508.pdf, last accessed August 14, 2024.

Zhao, J., Y. Li, H. Xu, and H. Liu. 2019. "Probabilistic Prediction of Pedestrian Crossing Intention Using Roadside LiDAR Data." *IEEE Access* 7: 93781–93790. https://doi.org/10.1109/ACCESS.2019.2927889, last accessed August 14, 2024.

Recycled
Recyclable

Recommended citation: Federal Highway Administration,
Enhancing Vulnerable Road User Detection and Volumetric Data Through Advanced Infrastructure Detection Technologies
(Washington, DC: 2025) https://doi.org/10.21949/1521784

HRSO-30/01-25(WEB)E